BIOCHEMISTRY
including biophysical chemistry & molecular biology

Article

pubs.acs.org/biochemistry

Diacyltransferase Activity and Chain Length Specificity of *Mycobacterium tuberculosis* PapA5 in the Synthesis of Alkyl β-Diol Lipids

Megan H. Touchette,[†] Gopal R. Bommineni,[†] Richard J. Delle Bovi,[‡] John E. Gadbery,[†] Carrie D. Nicora,[#] Anil K. Shukla,[#] Jennifer E. Kyle,[#] Thomas O. Metz,[#] Dwight W. Martin,[§,⊥] Nicole S. Sampson,[†] W. Todd Miller,[‡] Peter J. Tonge,[†] and Jessica C. Seeliger*[,∥]

Departments of [†]Chemistry, [‡]Physiology and Biophysics, [§]Medicine, and [∥]Pharmacological Sciences, [⊥]Proteomics Center, Stony Brook University, Stony Brook, New York 11790, United States

[#]Biological Sciences Division, Pacific Northwest National Laboratory, Richland, Washington 99352, United States

Supporting Information

ABSTRACT: Although they are classified as Gram-positive bacteria, Corynebacterineae possess an asymmetric outer membrane that imparts structural and thereby physiological similarity to more distantly related Gram-negative bacteria. Like lipopolysaccharide in Gram-negative bacteria, lipids in the outer membrane of Corynebacterineae have been associated with the virulence of pathogenic species such as *Mycobacterium tuberculosis* (Mtb). For example, Mtb strains that lack long, branched-chain alkyl esters known as dimycocerosates (DIMs) are significantly attenuated in model infections. The resultant interest in the biosynthetic pathway of these unusual virulence factors has led to the elucidation of many of the steps leading to the final esterification of the alkyl β-diol, phthiocerol, with branched-chain fatty acids known as mycocerosates. PapA5 is an acyltransferase implicated in these final reactions. Here, we show that PapA5 is indeed the terminal enzyme in DIM biosynthesis by demonstrating its dual esterification activity and chain-length preference using synthetic alkyl β-diol substrate analogues. By applying these analogues to a series of PapA5 mutants, we also revise a model for the substrate binding within PapA5. Finally, we demonstrate that the Mtb Ser/Thr kinases PknB and PknE modify PapA5 on three overlapping Thr residues and that a fourth Thr is unique to PknE phosphorylation. These results clarify the DIM biosynthetic pathway and indicate post-translational modifications that warrant further elucidation for their roles in the regulation of DIM biosynthesis.

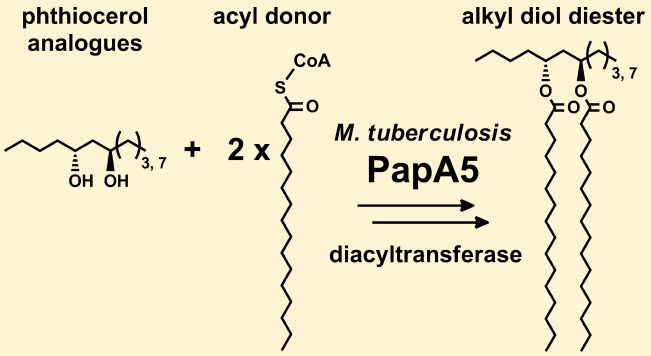

Bacteria that belong to the suborder Corynebacterineae are classified as Gram positive, but their cell wall is distinguished by long-chain fatty acids, known as mycolic acids, that are esterified to an underlying arabinogalactan carbohydrate layer.[1] In their covalent attachment to the cell wall, mycolic acids are analogous to the peptidoglycan-anchored wall teichoic acids of other Gram-positive bacteria,[2] but they constitute a unique, well-ordered layer that is believed to form the inner leaflet of a second lipid bilayer (sometimes referred to as the mycobacterial outer membrane or mycomembrane) that is distinct from the cytosolic membrane. The double-membrane structure of Corynebacterineae is analogous, therefore, to that of Gram-negative bacteria, which also possess an asymmetric outer membrane. In addition, just as lipopolysaccharide at the bacterial cell surface restricts cell permeability and plays key roles in host−pathogen interactions of Gram-negative bacteria,[3] noncovalently attached lipids in the outer membrane have been linked to the inherent drug resistance and virulence of pathogenic Corynebacterineae.[4]

Unsurprisingly, the more prominent examples of such virulence-associated lipids come from the human pathogen *Mycobacterium tuberculosis* (Mtb), whose outer membrane contains glycolipids and β-diol wax diesters that are unique to pathogenic strains. Of these, the dimycocerosates (DIMs) comprise two families of β-diol diesters that participate in Mtb−host interactions: phthiocerol dimycocerosates (PDIM) and the structurally related phenolic glycolipids (PGL).[5] Clinical Mtb strains that lack PDIM and mutants defective in PDIM biosynthesis or transport are attenuated for virulence in animal-based models of infection.[6−9] Diverse roles for PDIM in Mtb−host biology have been described[10−13] that underscore the importance of these unusual lipids in promoting the ability of Mtb to cause disease.

Received: April 25, 2015
Revised: August 12, 2015
Published: August 13, 2015

DOI: 10.1021/acs.biochem.5b00455
Biochemistry 2015, 54, 5457−5468

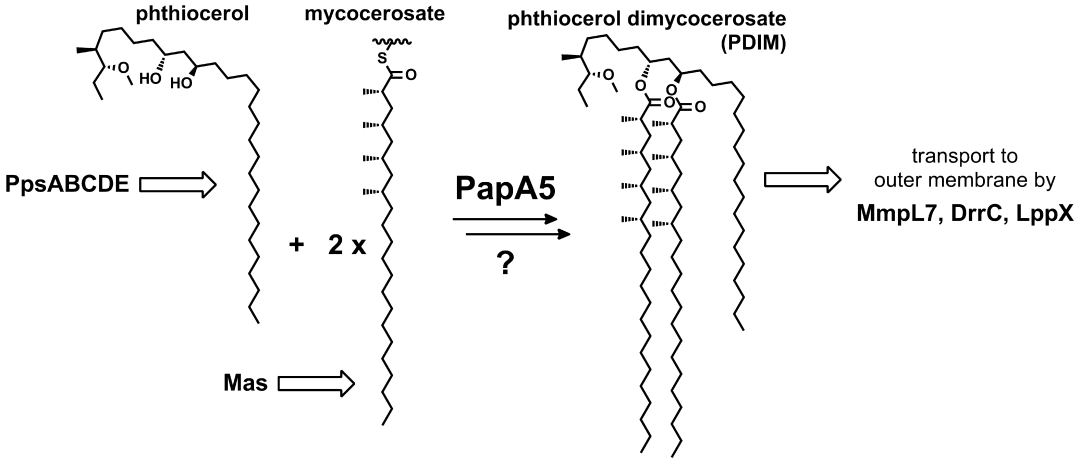

Figure 1. Biosynthesis of phthiocerol dimycocerosate (PDIM). The phthiocerol β-alkyl diol is synthesized by the modular polyketide synthase (PKS) PpsABCDE. The iterative PKS Mas generates mycocerosate, which is esterified directly onto the phthiocerol by PapA5 at least once. PapA5 may also be responsible for a second esterification that generates the final PDIM product, which is then transported to the outer membrane by MmpL7, DrrC and LppX.

Given the importance of DIMs in Mtb–host biology, DIM structure and biosynthesis have been extensively studied and recently summarized in a comprehensive review.[14] Briefly, both PDIMs (Figure 1) and PGLs comprise aliphatic β-diols, known as phthiocerols, esterified by long branched-chain fatty acids, known as mycocerosic acids. The PpsABCDE cluster of modular polyketide synthases (PKS) synthesizes phthiocerol β-diols. Pks1/15 makes the *p*-hydroxyphenylalkanoate precursor that FadD29 then passes to the Pps complex to form the phenolphthiocerol β-diol of PGL.[15] The mycocerosic acids are produced by another specialized PKS, mycocerosic acid synthase (Mas). Additional structural diversity within the DIM families arises from methoxy- and keto- versions of phthiocerol as well as variations in the length and number of branches in the mycocerosic chains.

The acyltransferase PapA5 has been implicated in the esterification of β-diols with mycocerosic acids to generate both PDIM (Figure 1) and PGL.[16,17] PapA5 has a preference for longer-chain (C_{12}–C_{18}) fatty acid-CoA substrates as acyl donors[17,18] and catalyzes the *in vitro* esterification of a variety of aliphatic alcohols, including vicinal and β-diols. When PapA5 was incubated with phenolphthiocerol, a putative native substrate isolated from *Mycobacterium leprae*, only a singly esterified product was detected,[16] leaving the ongoing question of whether PapA5 catalyzes successive reactions or, alternatively, a second and as yet uncharacterized acyltransferase follows PapA5 in DIM biosynthesis. Following synthesis in the cytosolic membrane, DIM localization in the outer membrane depends on the integral membrane transporters MmpL7 and DrrC and the cell wall lipoprotein LppX (Figure 1).[7,19,20]

There is precedent for dual esterification activity among acyltransferase related to PapA5. PapA5 belongs to an enzyme family that includes PapA1 and PapA2, which are involved in sulfoglycolipid biosynthesis, and PapA3, which initiates acyltrehalose biosynthesis.[21−23] Like DIMs, the products of these acyltransferases are surface-localized outer membrane lipids. PapA3 is unique in that it catalyzes two reactions and esterifies trehalose successively at the 1- and 2-positions with a straight-chain fatty acid and a branched-chain mycolipenic acid, respectively.[23] On the basis of this example, and the absence of any other predicted acyltransferase near the DIM biosynthetic locus, we hypothesized that PapA5 is indeed the sole acyltransferase in the DIM pathway.

Diverse conditions affect DIM production and PapA5 activity in Mtb, including carbon source, reductive stress, and transcriptional regulation in response upon macrophage infection.[24−28] PDIM biosynthesis may also be modulated by the activity of mycobacterial protein kinases. PDIM levels are attenuated in a PknH knockout strain, and *in vitro*, PknD modifies the PDIM transporter MmpL7 and PknB phosphorylates PapA5.[29−31] Phosphorylated peptides corresponding to Mas and Pks1/15 have also been detected in Mtb cell lysates.[32,33] We hypothesized that phosphorylation modulates PDIM biosynthesis, in part, via a direct effect on the catalytic activity of PapA5, as has been shown for other lipid biosynthetic enzymes in Mtb.[34−36]

Here, we present data that establish the dual esterification activity of PapA5 using synthetic β-diol substrate analogues and show that PapA5 has a preference for longer-chain β-diols. Using a series of mutations, we define the substrate-binding sites suggested by the previously published crystal structure and propose a model for the interaction of PapA5 with the phthiocerol and acyl donor substrates. We also show that PapA5 is a substrate for the Mtb kinases PknB and PknE. Phosphorylation by PknB and PknE overlaps at several Thr within an unresolved segment distal to the active site; modification by PknE was detected at one additional site.

EXPERIMENTAL PROCEDURES

Materials and Reagents. *Escherichia coli* XL-1 Blue (Stratagene) or Stellar (Clontech Laboratories) strains were used for cloning. *E. coli* BL21(DE3) cells were used for protein expression. Cells were grown in LB supplemented with 50 μg/mL kanamycin (for pET28b vectors) or 50 μg/mL streptomycin (for pCDFDuet-1 vectors) unless otherwise indicated. See Table S1 for details on vector constructs and oligonucleotide primer sequences. Alkyl alcohols (3*R*,5*R*)-heptane-3,5-diol and (3*S*,5*S*)-heptane-3,5-diol were purchased from Strem Chemicals, Inc. (Germany).

Synthesis of Alkyl *Anti*-β-Diol Compounds. *Overall Synthetic Scheme for 1,3-anti-β-Diols.* Compound **4** (Figure 3C) was synthesized as reported.[37,38] Compound **4** was coupled with hydroxylamine hydrochloride in the presence of

DOI: 10.1021/acs.biochem.5b00455
Biochemistry 2015, 54, 5457−5468

EDC/DIPEA to form **5**, which, upon reaction with the corresponding Grignard or lithium-derived agent, yielded **6** and **7** in good yield. Stereoselective reduction of compounds **6** and **7** with tetramethylammonium triacetoxyborohydride at −20 °C gave compounds **8** and **9**.

*(R)-3-Hydroxy-N-methoxy-N-methylheptanamide (**5**).*[38] *N,O*-Dimethylhydroxylamine hydrochloride (521 mg, 5.3 mmol, Acros Organics), EDC (1.73 mg, 9.0 mmol), *N,N′*-diisopropylethylamine (0.93 mL, 5.3 mmol, DIPEA, Alfa Aesar), and a catalytic amount of 4-dimethylaminopyridine (∼50 mg, 4-DMAP, Acros Organics) were added to a solution of compound **4** (600 mg, 4.1 mmol) in dry DMF. The mixture was stirred for 15 h at 24 °C and extracted with 10% HCl followed by a wash with saturated sodium bicarbonate. The extract was dried with magnesium sulfate, filtered, and evaporated under reduced pressure. The residue was purified by silica gel chromatography with petroleum ether/AcOEt (7:3, v/v) to obtain compound **5** (498 mg, 83% yield) as a white powder.

$[\alpha]_D^{23} = -58$ (*c* 1, CH_2Cl_2). ^{1}H NMR (500 MHz, $CDCl_3$): δ 3.86 (br s, 1H), 3.58 (br s, 1H), 3.55 (s, 3H), 3.04 (s, 3H), 2.51−2.31 (m, 2H), 1.38−1.16 (m, 6H), 0.75 (t, *J* = 7.2 Hz, 3H). ^{13}C NMR (125 MHz, $CDCl_3$): δ 173.4, 67.5, 60.8, 38.0, 36.0, 31.2, 27.3, 22.2, 13.5. MS (ESI^+) *m*/*z* (%): 190.1 (100) $[M + H]^+$.

*(R)-7-Hydroxyundecan-5-one (**6**).*[39] Compound **5** (203 mg, 1.1 mmol) was dried under argon and then reacted with 2 M *n*-butyl lithium in cyclohexane (1.5 mL, 18.2 mmol, Sigma-Aldrich) in dry THF under nitrogen at −78 °C for 2 h. The reaction mixture was extracted with saturated sodium bicarbonate, dried with magnesium sulfate, filtered, and evaporated under reduced pressure. The resulting residue was purified by silica gel chromatography with petroleum ether/AcOEt (4:1, v/v) to obtain compound **6** (137 mg, 68% yield) as a white powder.

$[\alpha]_D^{23} = -42$ (*c* 1, CH_2Cl_2). ^{1}H NMR (500 MHz, $CDCl_3$): δ 3.95 (br s, 1H), 3.31 (br s, 1H), 2.54−2.35 (m, 4H), 1.51−1.46 (m, 2H), 1.36−1.22 (m, 8H), 0.84 (m, 6H). ^{13}C NMR (125 MHz, $CDCl_3$): δ 212.2, 67.5, 48.9, 43.2, 36.1, 27.5, 25.5, 22.4, 22.1, 13.8, 13.6. MS (ESI^+) *m*/*z* (%): 169.2 (60), 187.2 (40) $[M + H]^+$.

*(5R,7R)-Undecane-5,7-diol (**8**; UDD).*[40,41] Tetramethylammonium triacetoxyborohydride (775 mg, 2.9 mmol, Sigma-Aldrich) was added to a stirred solution of acetonitrile (3.7 mL, 70.4 mmol, Fisher) and acetic acid (3.7 mL, 130 mmol, Fisher) at 24 °C. After 30 min, the reaction mixture was cooled to −78 °C and compound **6** (137 mg, 0.74 mmol) was added. The resulting mixture was stirred for 40 min followed by 36 h at −20 °C. The reaction mixture was extracted with saturated sodium bicarbonate, dried with magnesium sulfate, filtered, and evaporated under reduced pressure. The resulting residue was purified by silica gel chromatography with petroleum ether/AcOEt (4:1, v/v) to obtain compound **8** (36 mg, 26% yield) as a white powder.

$[\alpha]_D^{23} = -6.0$ (*c* 1, CH_2Cl_2). ^{1}H NMR (500 MHz, $CDCl_3$): δ 3.92 (t, J = 6.5 Hz, 2H), 2.57 (br s, 1H), 1.60−1.29 (m, 14H), 0.90 (t, *J* = 6.5 Hz, 6H). ^{13}C NMR (125 MHz, $CDCl_3$): δ 69.3, 42.3, 37.1, 22.6, 22.5 22.1, 14.0. MS (ESI^+) *m*/*z* (%): 189.2 (10), 169.2 (60) $[M + H]^+$.

*(R)-5-Hydroxypentadecan-7-one (**7**).*[39] Compound **5** (104.4 mg, 0.55 mmol) was dissolved in dry DMF under vacuum, 2 M octylmagnesium chloride in THF (0.6 mL, 3.2 mmol, Sigma-Aldrich) was added dropwise to the reaction mixture, and the reaction was cooled to −50 °C for 2 h. The reaction mixture was quenched with ammonium chloride, extracted with ethyl acetate twice, dried with magnesium sulfate, filtered, and evaporated under reduced pressure. The resulting residue was purified by silica gel chromatography with petroleum ether/AcOEt (4:1, v/v) to obtain compound **7** (70 mg, 67% yield) as a white powder.

$[\alpha]_D^{23} = -45$ (*c* 1, CH_2Cl_2). ^{1}H NMR (400 MHz, $CDCl_3$): δ 4.01 (br s, 1H), 3.05 (d, *J* = 3.2 Hz, 1H), 2.58 (dd, *J* = 17.6, 2.8 Hz, 1H) 2.51−2.39 (m, 3H), 1.60−1.26 (m, 18H), 0.91−0.85 (m, 6H). MS (ESI^+) *m*/*z* (%): 189.2 (10), 243.1 (80) $[M + H]^+$.

*(5R,7R)-Pentadecane-5,7-diol (**9**; PDD).*[40,41] Tetramethylammonium triacetoxyborohydride (304 mg, 1.2 mmol, Alfa Aesar) was added to a stirred solution of acetonitrile (1.45 mL, 27.5 mmol, Fisher) and acetic acid (1.45 mL, 50.7 mmol, Fisher) at 24 °C. After 30 min, compound **7** (70 mg, 0.29 mmol) was added and the reaction mixture was cooled to −78 °C for 40 min. The reaction was stirred at −20 °C for an additional 20 h. The reaction mixture was extracted with saturated sodium bicarbonate, dried with magnesium sulfate, filtered, and evaporated under reduced pressure. The resulting residue was purified by silica gel chromatography with petroleum ether/AcOEt (4:1, v/v) to obtain compound **9** (17 mg, 24% yield) as a white powder.

$[\alpha]_D^{23} = -5.0$ (*c* 1, CH_2Cl_2). ^{1}H NMR (400 MHz, $CDCl_3$): δ 3.94−3.90 (m, 2H), 2.40 (br s, 1H), 1.60 (t, *J* = 6.2, Hz, 2H) 1.52−1.26 (m, 22H), 0.92−0.85 (m, 6H). ^{13}C NMR (100 MHz, $CDCl_3$): δ 69.4, 42.2, 37.5, 37.1, 31.8, 29.6, 29.5, 29.2, 27.9, 25.7, 22.69, 22.65, 14.0. MS (ESI^+) *m*/*z* (%): 189.2 (10), 243.1 (80) $[M + H]^+$.

Synthesis of 3*R*,5*R*-Undecane-3,5-diol Dipalmitate (10) and 3*R*,5*R*-Pentadecane-3,5-diol Dipalmitate (11). Compounds **10** and **11** were synthesized from diols **8** and **9**, respectively, according to the protocol reported for PDIM A synthesis.[42,43] Compound **8** (10 mg, 53.11 μmol), palmitic acid (40.9 mg, 159.33 μmol, 3.0 equiv, Sigma-Adrich), DCC (43.8 mg, 212.44 μmol, 4.0 equiv) and DMAP (26.0 mg, 212.44 μmol, 4.0 equiv) were dissolved in dry DCM (0.5 mL), and the resulting mixture was stirred at 25 °C for 48 h under nitrogen. Compound **9** (10 mg, 41.08 μmol), palmitic acid (31.6 mg, 123.24 μmol, 3.0 equiv, Sigma-Aldrich), DCC (33.9 mg, 164.32 μmol, 4.0 equiv), and DMAP (20.1 mg, 163.32 μmol, 4.0 equiv) were dissolved in dry DCM (0.5 mL), and the resulting mixture was stirred at 25 °C for 48 h under nitrogen. For both reactions, the solvent was removed under reduced pressure, and the product was purified by silica gel chromatography with hexanes/ethyl ether (50:1, v/v) to obtain compound **10** (30 mg, 85.0% yield) or **11** (16.9 mg, 57.1% yield) as a white wax.

*3R,5R-Undecane-3,5-diol Dipalmitate (**10**).* ^{1}H NMR (400 MHz, $CDCl_3$): δ 4.92 (m, 2H), 2.27 (t, *J* = 8.0 Hz, 4H), 1.53−1.77 (m, 10H), 1.25−1.33 (m, 56H), 0.88−0.90 (m, 12H). ^{13}C (400 MHz, $CDCl_3$): δ 173.4, 70.1, 38.5, 34.6, 34.5, 31.9, 29.7, 29.6, 29.5, 29.4, 29.3, 29.2, 27.3, 25.0, 22.7, 22.6, 14.1, 14.0.

*3R,5R-Pentadecane-3,5-diol Dipalmitate (**11**).* ^{1}H NMR (400 MHz, $CDCl_3$): δ 4.92 (m, 2H), 2.27 (t, *J* = 7.2 Hz, 4H), 1.49−1.60 (m, 10H), 1.26−1.32 (m, 64H), 0.87−0.90 (m, 12H). ^{13}C (400 MHz, $CDCl_3$): δ 173.2, 70.0, 69.9, 38.3, 34.6, 34.4, 34.3, 31.8, 31.7, 29.6, 29.5, 29.4, 29.3, 29.2, 29.1, 29.0, 27.1, 25.0, 24.9, 22.6, 22.5, 22.4, 14.0, 13.8.

Cloning, Expression, and Purification of 6×His-PapA5. PapA5 (Rv2939) was cloned from H37Rv genomic DNA into pET28b (Novagen) via the NheI and HindIII restriction sites,

DOI: 10.1021/acs.biochem.5b00455
Biochemistry 2015, 54, 5457−5468

and a TEV protease cleavage site was inserted at the N-terminus before the 6×His tag (Table S1). To investigate the putative substrate binding channels, the following mutations were made in the pET28b 6×His-TEV-PapA5 vector by site-directed mutagenesis using overlapping primers (Table S1): G129L, S380M, S380F, A382M, Q19R, and Q19K as well as V16C/G328C (generated with two successive mutagenesis reactions). The sequence-verified pET28b 6×His-TEV-PapA5 constructs were transformed into *E. coli* BL21(DE3) cells. N-terminally 6×His-tagged PapA5 was expressed and purified as described.[17] PapA5 aliquots were snap frozen in 50 mM Tris, pH 7.4, 100 mM NaCl, 1 mM DTT, 10% glycerol and stored at −80 °C.

Isotope-Coded Mass Tagging. PapA5 (V16C/G328C) (70 μM) was allowed to thaw on ice. A 50 μL reaction containing 12 μM PapA5 (V16C/G328C), 50 mM HEPES, pH 7, and 1% (w/v) sodium deoxycholate (SDC) was prepared at 25 °C before the addition of 5 mM 4-(2,5-dioxo-2*H*-pyrrol-1(5*H*)-yl)-*N*,*N*,*N*-trimethyl-*d*9-butan-1-aminium iodide.[44] After incubating for 10 min at 25 °C, excess label was removed by adding 450 μL of 50 mM HEPES, pH 7, and centrifuging for 6 min at 12 000*g* in a centrifugal filter (Amicon Ultra 0.5 mL 10k MWCO, Millipore). The wash step was repeated four more times to reduce the label concentration to 0.5 μM. Tris(2-carboxyethyl)phosphine (TCEP, 4.5 mM final concentration) was added to the retentate, and the solution was incubated for 2 h at 25 °C. The TCEP concentration was reduced to 5 μM by centrifugal washing and filtration as above. The reduced protein was incubated with 5 mM 4-(2,5-dioxo-2*H*-pyrrol-1(5*H*)-yl)-*N*,*N*,*N*-trimethylbutan-1-aminium iodide[44] and 1% SDC for 10 min at 25 °C and then for 1 h at 70 °C. The labeled protein was digested with chymotrypsin (10 ng/μL final concentration), and the solution was incubated for 16 h at 25 °C. To quench the digestion and precipitate the SDC, 3.5% (v/v final concentration) trifluoroacetic acid (TFA) was added and the mixture was incubated for 10 min at 25 °C. The precipitate was removed by centrifugation for 10 min at 18 000*g*. The supernatant containing the digested peptides was recovered, and an equal volume of supernatant and 2,5-dihydroxybenzoic acid (DHB) matrix were mixed and immediately spotted for peptide fingerprint analysis by MALDI-TOF (Bruker Auto-FlexII).

PapA5 Enzymatic Reactions. Reactions contained 2 μM PapA5, 18 μM [1-^{14}C]palmitoyl-CoA (PerkinElmer), and 180 μM OCT, UDD, or PDD or 100 mM heptanediol in 25 μL of reaction buffer (MES, pH 6.5, 100 mM NaCl). Reactions were initiated by the addition of PapA5, incubated for 12−16 h at 20−25 °C, and quenched with an equal volume of ethanol. Specific activity was determined from reactions incubated at 20−25 °C for 45 min. A 2 μL aliquot of each quenched reaction was spotted on silica thin-layer chromatography (TLC) plates (high-performance TLC Silica Gel 60; EMD Chemicals) and developed in 3:1 hexanes/ethyl acetate. For biphasic reactions, immediately after all components were combined, twice the reaction volume of hexanes was added slowly as a separate phase on top of the aqueous reaction mixture. Biphasic reactions were not quenched; instead, 3 μL of the hexanes layer was spotted for TLC. All TLC plates were visualized by phosphorimaging, and densitometry analysis was performed using ImageJ software. For isolation of monoester PDD, a 1.25 mL reaction contained 2 μM PapA5, 18 μM [1-^{14}C]palmitoyl-CoA, and 420 μM PDD in reaction buffer and was incubated for 16 h at 25 °C. The reaction was spotted on a TLC plate and developed in 85:15 hexanes/ethyl acetate. The silica containing monoester product was scraped off the plate, and the monoester product was extracted from the silica with hexanes. The resulting monoester product was incubated with 2 μM PapA5 and 18 μM [1-^{14}C]palmitoyl-CoA for 16 h at 25 °C. The reactions were spotted and TLC developed in 3:1 hexanes/ethyl acetate.

Mass Spectrometry Analysis of PapA5 Reactions. Biphasic reactions contained 2 μM PapA5, 18 μM palmitoyl-CoA, and 180 μM phthiocerol analogue in 500 μL of reaction buffer with 1 mL of hexanes overlaid on the aqueous reaction mixture. The hexanes layer was removed after 12−16 h incubation at 20−25 °C and allowed to evaporate to dryness. The resulting film was resolubilized in 12 μL of 2-propanol per sample and analyzed by UPLC-ESI-MS as previously described.[45]

Kinase Phosphorylation Assays. Mtb kinases Pkn B, D, E, H, K and L were purified as His-tagged fusions to maltose-binding protein (MBP-Pkn) and were a kind gift of Dr. Christina Baer.[46] Radiolabeled phosphorylation reactions contained 2.8 μM PapA5, 1 μM MBP-PknB. Final reaction volumes were 25 μL and contained 20 mM PIPES, pH 7.2, 5 mM $MgCl_2$, 5 mM $MnCl_2$, 400 μM ATP, and 10 μCi [γ-^{32}P]-ATP (PerkinElmer, 10 mCi/mL). Reactions were incubated at 30 °C for 20 min and were quenched by the addition of SDS-PAGE sample buffer with DTT. The reactions were analyzed by SDS-PAGE (12% acrylamide) with Coomassie blue staining. After drying, the gels were analyzed by autoradiography (22 h exposure). For the kinase activity screen with Pkn B, D, E, H, K, and L, radiolabeled phosphorylation reactions contained 1 μM MBP-Pkn (all variants) and 1 μM PapA5 or myelin basic protein (MyBP). Final reaction volumes were 50 μL and contained 50 mM Tris (pH 7.4), 5 mM $MgCl_2$, 5 mM $MnCl_2$, 50 μM ATP, and 1 μCi [γ-^{32}P]-ATP (PerkinElmer, 10 mCi/mL). Reactions were incubated at 30 °C for 1 h and quenched by the addition of SDS-PAGE sample buffer. Proteins were loaded and separated by SDS-PAGE (8% acrylamide for PapA5 gel; 12% acrylamide for MyBP gel), stained, and analyzed as above (24 h exposure).

Coexpression with Pkn and Purification of 6×His-PapA5. The PknB (Rv0014c) catalytic domain (amino acids 1−330) was cloned from Mtb H37Rv genomic DNA into pCDFDuet-1 (Novagen) via the NdeI and KpnI restriction sites (Table S1). PknE (Rv1743; aa 1−290) was similarly cloned into pCDFDuet-1 (Table S1). PknB and PknE expressed from the final vectors are untagged. The sequence-verified constructs pCDFDuet PknB 1−330 and PknE 1−290 were each transformed into *E. coli* BL21(DE3) containing pET28b 6×His-TEV-PapA5. Double-transformed cells were grown in LB broth (Neogen) with 30 μg/mL streptomycin and 30 μg/mL kanamycin. Cultures were grown at 37 °C with shaking at 250 rpm to an OD_{600} of 1.0, induced with 1 mM isopropyl-β-D-thiogalactopyranoside, and incubated for an additional 4 h. Cells were lysed in 20 mM Tris, pH 7.4, 200 mM NaCl, 15 mM imidazole, 1 mM EDTA, 1 mM DTT (lysis buffer). The clarified crude lysate was incubated with Ni-NTA agarose resin (Qiagen) for 30 min at 4 °C. The resin was subsequently washed with 10 resin volumes of lysis buffer and 15 resin volumes of 50 mM Tris, pH 7.4, 100 mM NaCl, 1 mM DTT, 10% glycerol (storage buffer) with 15 mM imidazole. PapA5 was eluted in storage buffer with 250 mM imidazole. Fractions containing purified PapA5 were pooled and dialyzed overnight at 4 °C into storage buffer. PapA5 was coexpressed

DOI: 10.1021/acs.biochem.5b00455
Biochemistry 2015, 54, 5457−5468

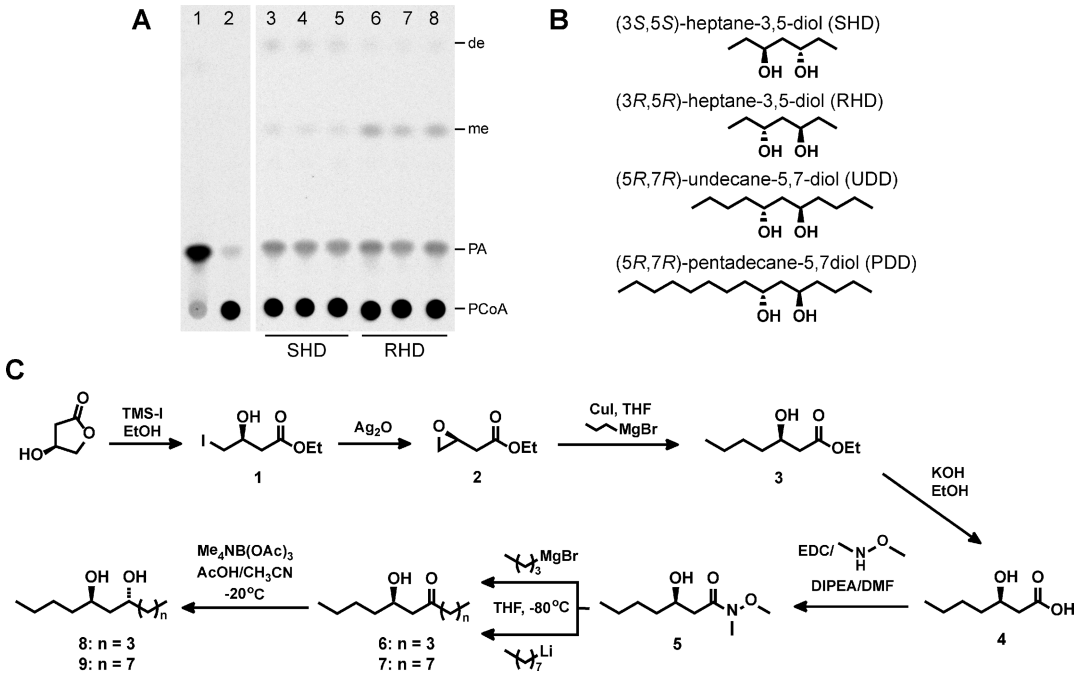

Figure 2. Substrate analogues recapitulate phthiocerol diol regio- and stereoselectivity. (A) PapA5 (2 μM) was incubated overnight with 18 μM [^{14}C-1]-palmitoyl-CoA (PCoA) and 100 mM 3*S*,5*S*-heptane-3,5-diol (SHD; lanes 3−5) or 3*R*,5*R*-heptane-3,5-diol (RHD; lanes 6−8). The migration of the diesters (de) and monoesters (me) are indicated. Triplicate reactions for each substrate are shown. Products were analyzed by TLC (3:1 hexanes/ethyl acetate) and analyzed by phosphorimaging visualization and densitometry. PCoA and [1-^{14}C]-palmitic acid (PA; product of competing PCoA hydrolysis) were included as migration standards (lanes 1 and 2). (B) Structures of SHD, RHD, and the longer-chain analogues 3*R*,5*R*-undecane-5,7-diol (UDD) and 3*R*,5*R*-pentadecane-5,7-diol (PDD). (C) Synthetic scheme for UDD (**8**) and PDD (**9**).

with PknE under the same conditions as above with PknB. The protocol for purification under denaturing conditions was adapted from the Qiagen manual (The QIA Expressionist 6/2013). Buffers used for the purification were variations on 100 mM NaH_2PO_4, 10 mM Tris, 8 M urea. Buffer D1 was adjusted to pH 8.0, buffer D2 was adjusted to pH 6.3, buffer D3 was adjusted to pH 5.9, and buffer D4 was adjusted to pH 4.5. The cells were resuspended in 5 mL buffer D1 per 1 g of cell pellet weight and stirred for 30 min at 25 °C. Cells were then lysed by sonication, and the lysate was spun for 30 min at 10 000*g* to pellet unbroken cells. Lysates were incubated with Ni-NTA resin equilibrated in buffer D1 (1 mL resin slurry per 4 mL lysate) for 60 min at 25 °C. Resin was pelleted at 1000*g* for 2 min to removed flow through. The resin was then washed with 1 × 5 mL buffer D1 and 3 × 5 mL buffer D2. PapA5 was eluted from the resin in 3 × 1 mL buffer D3 and 3 × 1 mL buffer D4, and fractions 1−5 were pooled and concentrated using a 30 kDa MWCO concentrator (Millipore).

Mass Spectrometry Analysis of Purified PapA5. PapA5 purified as above was diluted in 100 mM ammonium bicarbonate, reduced with 4 mM DTT, and alkylated with 8.4 mM iodoacetamide. The protein was then digested with trypsin (Trypsin Gold, mass spectrometry grade, Promega, USA) at a 25:1 protein/trypsin mass ratio for 16 h at 37 °C. The digests were brought to 2% (v/v) formic acid (FA) and desalted with Supel-Tips C18 micropipette tips (Sigma-Aldrich) using FA-containing solutions containing varying proportions of acetonitrile (ACN) according to the vendor's instructions. Eluted peptides were dissolved in 2% ACN, 0.1% FA (buffer A) for analysis on an LTQ Orbitrap XL ion trap mass spectrometer (Thermo Fisher, San Jose, CA) equipped with a nanoliquid chromatography electrospray ionization source. The peptides were eluted at 300 nL min^{-1} from a homemade 5 μm ProntoSil 120-5-C18H (Bischoff Chromatography, Leonberg, Germany) capillary column [2% buffer B (98% ACN, 0.1% FA) to 40% buffer B over 115 min; 40 to 80% buffer B over 3 min and held for 3 min; 80 to 2% buffer B over 0.1 min and held for 29 min]. Full mass spectra (MS) were recorded over m/z 400 to 2000, 60 000 resolution, followed by top-five MS/MS scans in the ion trap. Peptides with a charge/state of +2 or higher were analyzed. MS/MS spectra were extracted from the RAW file with ReAdW (http://sourceforge.net/projects/sashimi). The resulting mzXML data files were searched with Inspect against a custom database composed of the UniProt EColi_K12 proteome with added sequences for the expressed PapA5 proteins and common contaminants. The data were also analyzed using the GPM X! Tandem and MaxQuant Andromeda search engines.

RESULTS

PapA5 Activity with Alkyl-1,3-diol Substrates. The substrate specificity of PapA5 has been probed previously with an array of commercially available alkyl alcohols that included primary aliphatic alcohols (C_2−C_{20}), tertiary alcohols (2-alkyl alcohols, C_6 and C_8) and both vicinal and β-diols (C_6−C_{10}).[17,18] Of these, the highest activity was observed with the primary aliphatic alcohol 1-octanol (OCT). In comparison, all diols showed at least 5-fold less product formation under the same conditions, although even with these low levels of activity a proportion of diester was observed (2−4% compared to OCT product formation).[17] Given the strong preference for primary alkyl alcohols over diol substrates, the question of whether dual esterification is a physiological function for PapA5 still remained.

We hypothesized that PapA5 discriminates both the relative position of the two hydroxyl groups and the chain length on

DOI: 10.1021/acs.biochem.5b00455
Biochemistry 2015, 54, 5457−5468

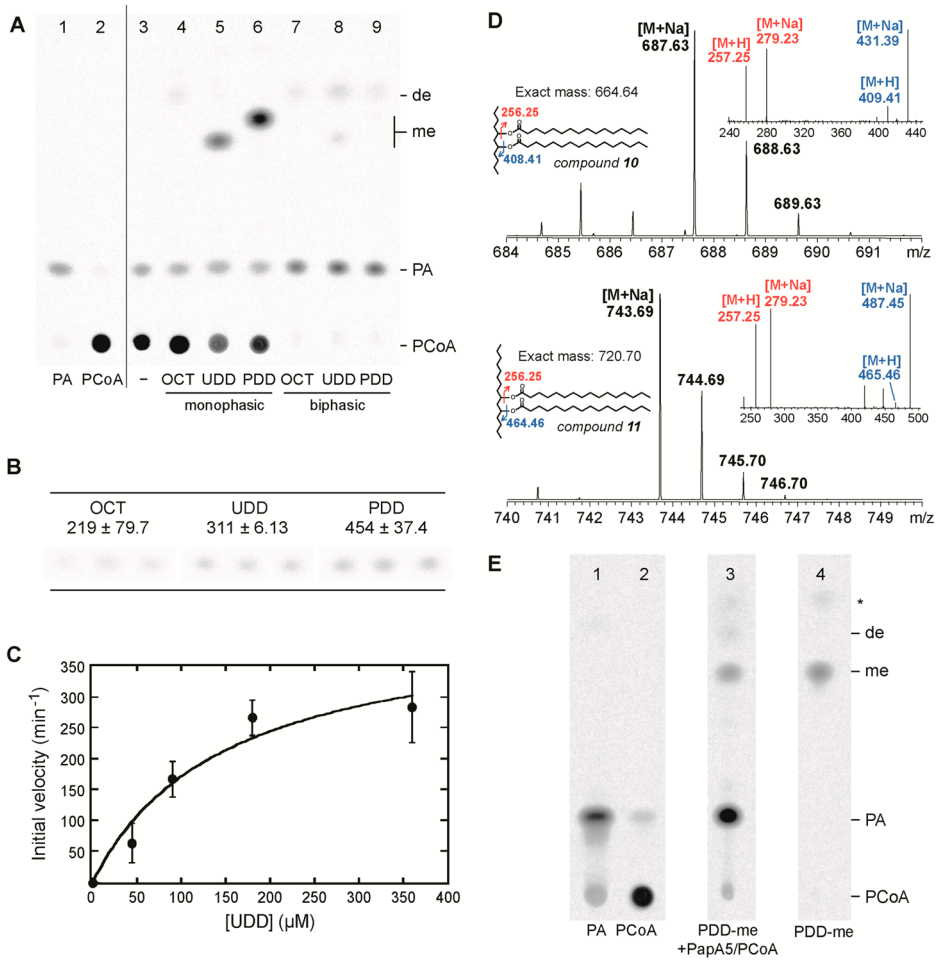

Figure 3. PapA5 diacylates β-diol substrates and prefers longer-chain substrates. (A) PapA5 was incubated overnight with 18 μM [1-^{14}C]-PCoA and DMSO vehicle (lane 3) or 180 μM of the indicated substrate analogues under monophasic aqueous conditions (lanes 3–6) or biphasic buffer/hexanes conditions (lanes 7–9; only organic phase spotted). Products were analyzed as in Figure 2A. Palmitoyl-OCT and the diesters (de) of UDD and PDD have similar R_f values in this mobile phase. Monoesters (me) of UDD and PDD are also indicated. OCT served as a positive control for PapA5 activity. Data are representative of three replicate experiments. (B) Specific activity for monoester formation is in μM min^{-1} mg^{-1} PapA5 at 18 μM [1-^{14}C]-PCoA and 180 μM of the indicated substrate under monophasic conditions (22 °C, 45 min.). Activities are the average of three replicates (shown) ± SD. (C) Initial velocity of palmitoyl-UDD formation as a function of UDD concentration (K_m = ~150 μM, k_{cat} = 2.84 μM^{-1} min^{-1}). (D) The diacyl products from biphasic reactions with UDD (left) and PDD (right) were confirmed by UPLC/ESI-tandem mass spectrometry in positive mode. The sodium adduct ion was observed at the predicted m/z for both substrates (top row). MS2 analysis (bottom row) of the m/z 687.63 and 743.69 parent ions confirmed fragmentation at the ester bond (R = $-C_{15}H_{31}$). (E) Reactions were performed as in (A) except PapA5 was incubated with PDD-[1-^{14}C]-monopalmitate (PDD-me) and PCoA (lane 3; only the organic phase was spotted). PA and PCoA (lanes 1 and 2 in both A and B) and TLC-purified PDD-me (lane 3 in B) served as migration standards. The asterisk indicates an impurity carried over from purified PDD-me.

either side of the β-diol. We therefore tested PapA5 activity with the commercially available 3*S*,5*S*- and 3*R*,5*R*-heptanediols (SHD and RHD, respectively) since they are longer than previously tested 2,4-pentanediols, which were not esterified.[17] PapA5 was expressed and purified as previously described, and purity was confirmed by Coomassie stain (Figure 4A) and tryptic digest LC-MS/MS (>90% spectral counts assigned to PapA5). When incubated with PapA5 and ^{14}C-palmitoyl-coenzyme A (PCoA) as the acyl donor, products consistent with the monoester and diester were detected by thin-layer chromatography (TLC) only at substrate concentrations 200 times higher than the K_m of 0.5 mM for OCT (Figure 2A).[17] Therefore, the data from these substrates did not support diesterification as a native function of PapA5. Interestingly, RHD, which has the same stereochemistry as phthiocerol, gave a higher yield of monoester (6.7 ± 1.2% of input for RHD vs 1.9 ± 0.24% for SHD), suggesting that PapA5 can discriminate substrate stereochemistry at the first acylation step.

We then synthesized the analogues 5*R*,7*R*-undecane-5,7-diol (UDD) and 5*R*,7*R*-pentadecane-5,7-diol (PDD) to recapitulate the stereochemistry of the native phthiocerol and to extend the chain length (Figure 2B,C). The desired anti stereochemistry was obtained using well-documented methods for the reduction of the β-*R*-hydroxy ketone precursor with high diastereoselectivity (~95:5 anti/syn) (Figure 2C).[47]

Under previously reported aqueous buffer conditions,[17] both UDD and PDD yielded a single product spot by TLC (Figure 3A, lanes 4–6). However, mass spectrometry confirmed that these products were the monoester forms (data not shown). Nevertheless, these conditions revealed that PapA5 has a higher specific activity with UDD and PDD than with OCT and also prefers the longer-chain PDD over UDD for formation of the monoester (Figure 3B). Also, the apparent K_m for UDD (~150

DOI: 10.1021/acs.biochem.5b00455
Biochemistry 2015, 54, 5457–5468

Table 1. Specific Activities of PapA5 Mutants for Formation of the Monoester

mutation(s)	specific activity (μM min^{-1} mg^{-1})					
	OCT		UDD		PDD	
wild type[a]	219 ± 79.7		311 ± 6.13		454 ± 37.4	
G129L	28.2 ± 7.2	(**13%**)[b]	11.4 ± 3.3	(**4%**)	58.8 ± 17.5	(**13%**)
S380M	<5.0		<5.0		<5.0	
A382M	76.0 ± 7.7	(**35%**)	121 ± 12.1	(39%)	220 ± 16.1	(48%)
A382F	<5.0		<5.0		18.7 ± 14.9	(**4%**)
Q19R	150 ± 14.6	(68%)	150 ± 10.4	(48%)	249 ± 36.7	(55%)
Q19K	35.8 ± 6.5	(**16%**)	<5.0		50.4 ± 10.5	(**11%**)
V16C/G328C	<5.0		26.1 ± 9.5	(**8%**)	13.6 ± 7.0	(**3%**)

[a]Raw data is shown in Figure 3B. [b]Percent wild-type activity. Mutants that displayed less than 20% wild-type activity for all substrates are indicated in bold.

μM) was 3-fold lower than that for OCT (500 μM), and the k_{cat} for UDD was 4 orders of magnitude faster (2.84 μM^{-1} min^{-1} vs 4.4 × 10^{-5} μM^{-1} min^{-1}) (Figure 3C). In contrast, at PDD concentrations ≥360 μM, the diester product was detected, indicating that under these conditions monoester competes with PDD for binding to PapA5 (Figure S1). Thus, the Michaelis−Menten steady-state assumption no longer holds, and the rate of monoester formation could not be directly determined for the longer-chain PDD substrate. Nevertheless, the results with UDD still underscore that, unlike previously tested substrates, PapA5 is significantly more active with UDD than OCT.

We hypothesized that the hydrophobicity of the monoester product leads to aggregation that hinders access by PapA5 and inhibits diester formation. This could also explain why only the monoester product was observed when PapA5 was incubated with phenolphthiocerol.[16] We therefore screened PapA5 activity with PDD in a series of phase-separated aqueous−organic systems (1:2 buffer/solvent, where the solvent was diethyl ether, chloroform, ethyl acetate, heptanes, or hexanes) and found that the highest, most reproducible yield of PDD diester was obtained with hexanes (data not shown). We further verified that PapA5 activity with OCT was similar in aqueous and biphasic buffer/hexanes conditions and that PapA5 is therefore not adversely affected by the inclusion of the organic layer (Figure S2). Therefore, buffer/hexanes (1:2) was used for all subsequent experiments. Under these conditions, additional products with higher R_f for both UDD and PDD were observed by TLC (Figure 3A, lanes 8 and 9) and confirmed as the predicted dipalmitate products using tandem mass spectrometry (Figure 3D) and comparison to synthetic UDD-dipalmitate (**10**) and PDD-dipalmitate (**11**) standards (data not shown). Finally, PDD-1-^{14}C-monopalmitate was isolated by preparative TLC and shown to be a substrate for PapA5, thereby confirming that PapA5 successively esterifies the alkyl diol to form the diester (Figure 3E).

Analysis of Mutations That Affect Substrate Binding to PapA5. On the basis of the PapA5 crystal structure and its similarity to other acyl-CoA-dependent acyltransferases, Buglino et al. described two putative substrate-binding channels and hypothesized that the channels accommodate the two arms of phthiocerol with the hydroxyl nucleophiles positioned near the active site (Figure S3A).[18] We therefore predicted that bulky mutations at different locations along channel 1 would differentially affect the turnover of OCT, UDD, and PDD based on their chain lengths, whereas a bulky mutation in the predicted pantetheine-binding channel should have the same effect for all substrates (Figure S3A). Buglino et al. also noted that an additional helix, helix H, shortens channel 2 in PapA5 relative to that of related acyltransferases and proposed that this helix must move to allow phthiocerol to bind. Thus, mutations designed to constrain helix H by forming a salt bridge or disulfide bond with the adjacent helix A would be predicted to decrease turnover of UDD and PDD but not OCT since this primary alcohol would not require access to channel 2 (Figure S3A).

To test these predictions, we created a series of mutations (Figure S3A). The purified mutant proteins were all soluble and isolated in good yield, and the mutations did not have a significant effect on the overall PapA5 protein fold, as indicated by circular dichroism spectra (Figure S4). As predicted, G129L, which introduces steric hindrance in the pantetheine-binding channel and would therefore affect PCoA binding, reduced PapA5 activity for the three substrates (Table 1). In channel 1, S380M completely abrogated activity for all substrates, consistent with the proximity of this position to the active site (~12 Å from H124, which is required for activity and thought to serve as a catalytic base[17]). However, contrary to predictions, the effects of all other mutations also did not vary with substrate. For example, A382 is ~15 Å from H124, and a bulky side chain would be expected to hinder PDD (~12 Å for the longer arm) and OCT (~11 Å) but not UDD (~7.5 Å). Although mutation of A382 to Phe had a more severe effect on activity than mutation to Met, the level of catalytic impairment of each mutant was similar to all three substrates. For mutations designed to constrain helix H, mutation of Q19 to Lys reduced activity more than mutation to Arg, suggesting that Lys is more effective at forming a salt bridge with E332 and thereby constraining helix H than Arg. The double-cysteine mutant V16C/G328C forms a disulfide bond between these two residues on helices A and H, as verified by the dependence of isotope-labeled maleimide modification upon treatment with reducing agent (Figure S3B).[44] The effect of the disulfide bond on PapA5 activity was more severe than that for the salt bridge Q19K mutation, but again, the reduction in catalytic activity was similar across all substrates.

Phosphorylation of PapA5 by Mtb Ser/Thr Kinases. Recently, biosynthetic enzymes involved in mycolic acid biosynthesis have been shown to be phosphorylated by Ser/Thr kinases with consequent downregulation of catalytic activity. For example, phosphorylation of the fatty acid synthase II (FASII) enoyl-ACP reductase InhA reduces activity by lowering the affinity for the NADH cofactor.[34] Inhibition of β-ketoacyl acyl carrier protein synthase KasB upon phosphorylation is attributed to the proximity of the modified Thr residues to the catalytic triad.[36] Since PDIM levels are

DOI: 10.1021/acs.biochem.5b00455
Biochemistry 2015, 54, 5457−5468

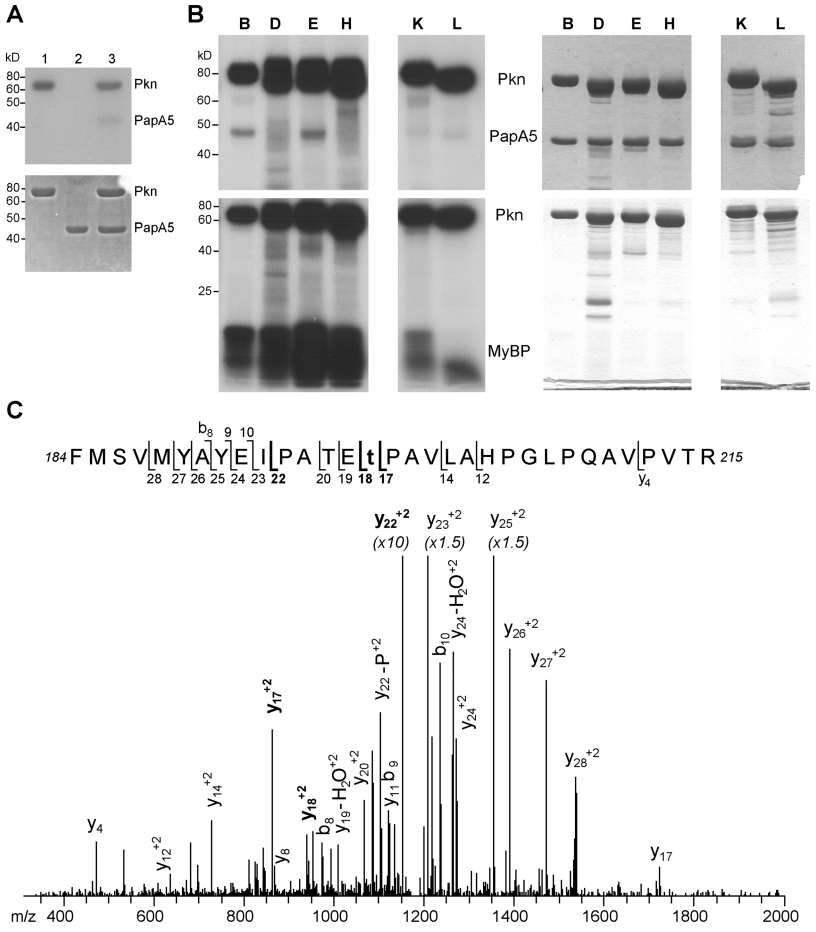

Figure 4. PknB and PknE phosphorylate PapA5. Mtb Pkn kinase domains were purified as fusions to MBP and incubated with γ-^{32}P-ATP. (A) PknB autophosphorylates (lane 1), and PapA5 is phosphorylated only in the presence of PknB (lane 3). Autoradiogram (24 h exposure; top) and Coomassie-stained SDS-PAGE gel (bottom). (B) PknB, D, E, H, K, and L were each incubated with PapA5 (top) or myelin basic protein as a positive control (MyBP; bottom). Autoradiogram (24 h exposure; left) and Coomassie-stained SDS-PAGE (right). Approximate MW: MBP-Pkn, ~80 kDa; PapA5, 49 kDa; MyBP, 18 kDa. (C) An example MS2 spectrum for the aa 184−215 peptide of PapA5 coexpressed with PknB shows phosphorylation of T198 (indicated by **t** in the peptide sequence). The triply charged ion has predicted m/z 1179.58 (monoisotopic) and m/z 1180.36 (avg); the parent ion was detected at m/z 1180.25. Phosphorylation at T198 is supported by the peak for **y18** and the strong proline peaks for **y17** and **y22**.

modulated by growth conditions, infection, or the presence of PknH, we hypothesized that Mtb Ser/Thr kinases may also regulate PDIM production by modifying PapA5. We first confirmed that PapA5 is phosphorylated only in the presence of kinase and [γ-^{32}P]-ATP and thereby confirmed that PapA5 is a substrate for PknB, as previously observed (Figure 4A).[31] We then tested Pkn D, E, H, K, and L for their ability to phosphorylate PapA5 as well. All kinases were active, as demonstrated by autophosphorylation and phosphorylation of myelin basic protein (MyBP), a model substrate that is phosphorylated by many Mtb Ser/Thr kinases,[48,49] but only PknB and PknE phosphorylated PapA5 (Figure 4B).

PknB phosphorylation of threonines on PapA5 has been reported, but the location and functional consequences of the modification have not been examined.[31] To determine the effect of phosphorylation on catalytic activity, PapA5 was isolated from *E. coli* cells coexpressing the PknB kinase domain, but no change in activity was detected relative to that of unmodified PapA5 using OCT, UDD, or PDD as substrates (data not shown). To verify phosphorylation by PknB and determine the site(s) of modification, PapA5 was analyzed by tandem mass spectrometry. PapA5 expressed by itself showed no evidence for phosphorylation, as determined by three independent search programs (MaxQuant, InsPecT, and GPM X! Tandem). In contrast, phosphorylation was detected in PapA5 isolated from PknB coexpressing cells. Specifically, both MaxQuant and InsPecT detected phosphorylation on the peptide aa 184−215. Although quantification of the degree of phosphorylation was not possible, manual inspection of the MS2 spectra confirmed peptides with modification at T196, T198, or T214. A representative spectrum for phosphorylation at T198 is shown in Figure 4C.

PknE phosphorylation of PapA5 has not been previously reported. Upon coexpression with PknE, PapA5 was insoluble. PapA5 expressed by itself and coexpressed with PknE was isolated in parallel under denaturing conditions and subjected to tandem mass spectrometric analysis as above. Both MaxQuant and GPM X! Tandem detected phosphorylation at T196, T198, and T214, suggesting overlap with PknB phosphorylation sites. One additional phosphorylation site at T144 was detected by both algorithms (Figure 5C). T144 is located at the end of helix C, the N-terminus of which forms part of the active site. The T144 side chain hydroxyl is appropriately positioned to form a hydrogen bond with the

DOI: 10.1021/acs.biochem.5b00455
Biochemistry 2015, 54, 5457−5468

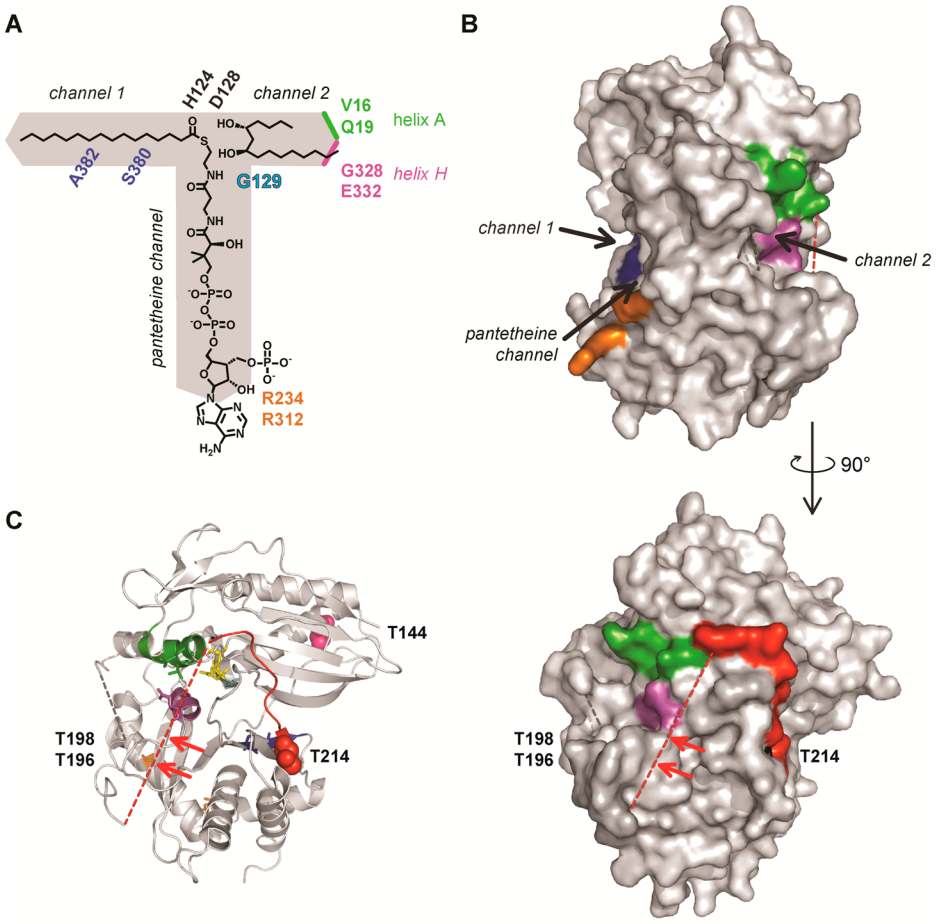

Figure 5. Model for PapA5 substrate binding and protein interactions. (A) Modified schematic of the substrate channels showing the proposed binding modes for the acyl acceptor (here, palmitate) in channel 1 and the alkyl diol (PDD) in channel 2. (B) PapA5 crystal structure (PDB ID: 1Q9J) showing the apposition of the Mas-ACP-interacting residues R234 and R312 (orange) and helices H and A. Dashed lines designate unresolved regions. (C) The region highlighted in red encompasses residues T196, T198, and T214 that are phosphorylated by both PknB and PknE. Residue T144 (pink) is also phosphorylated by PknE. Arrows indicate the approximate positions of T196 and T198. Catalytic residue H124 and active-site residue D128 are shown in yellow.

backbone amide proton of T355 (T144 hydroxyl O to T355 amide N atom-to-atom distance, 3.3 Å). PknE phosphorylation of T144 may disrupt this interaction and destabilize PapA5, leading to the insolubility and aggregation observed upon coexpression in *E. coli*.

DISCUSSION

Our observation that PapA5 catalyzes dual esterification with a preference for longer-chain β-diols provides strong support for the assignment of PapA5 as a diacyltransferase and the final enzyme in DIM biosynthesis (Figure 1). Furthermore, the results of our mutational analysis are not consistent with the previously reported model for substrate binding to PapA5 and suggest that a revised model is required. Indeed, after the structure of PapA5 was reported, structures of mammalian carnitine acyltransferases in complex with CoA, carnitine, or substrate-competitive inhibitors revealed that channel 1 accommodates the alkyl chain of the acyl-CoA substrate with the electrophilic center at the active site, whereas channel 2 binds to the carnitine nucleophile.[50−53] In line with these structures and our activity data, we propose that in PapA5 mycocerosic acid binds to channel 1 and phthiocerol binds to channel 2 (Figure 5A). None of the mutants in channel 1 (S380M, A382M/F) showed significant discrimination among OCT, UDD, and PDD substrates despite the varying chain lengths, suggesting that channel 1 does not bind to the diol substrate but rather accommodates the alkyl chain of the acyl donor. In this model, constraining helix H affects substrates of all chain lengths equally, as observed, since helix H is only ~7 Å from the active site H124. Major structural rearrangements proximal to helix H would be required, therefore, to position the hydroxyl nucleophile(s) at the active site while accommodating the two arms of phthiocerol. Flexibility in this region of PapA5 is suggested by regions around helix H that are unresolved in the crystal structure (aa 176−180 and aa 192−204).[18] For the second esterification, channel 2 may accommodate the mycocerosate chain as well as the phthiocerol of the monoester substrate. Given the size of phthiocerol monomycocerosate, channel 1 may also be required to bind to the monoester, although this possibility could not be determined from the existing mutants and activity data.

Our revised model for substrate binding, in which phthiocerol and mycocerosic acid occupy distinct channels that orient the nucleophile and electrophile in the active site at the channel junction, implies that phthiocerol is only partially bound by PapA5. Even if helix H moves away, channel 2 is too

DOI: 10.1021/acs.biochem.5b00455
Biochemistry 2015, 54, 5457−5468

shallow (~11 Å from H124 to the surface) to accommodate the longer arm (C_{21}–C_{24}) of phthiocerol. Moreover, for the second esterification reaction PapA5 must access the unmodified hydroxyl on the highly hydrophobic phthiocerol monomycocerosate. Our results also show that for efficient diester synthesis PapA5 requires a hydrophilic–hydrophobic interface, which in Mtb could be provided by the cytosol–membrane interface. Although PapA5 is soluble, it may be proximal to the membrane in Mtb, consistent with other soluble biosynthetic enzymes that act on lipid intermediates in cell wall biosynthesis and have been localized to polar sites of cell wall growth.[54,55]

PknB and PknE Phosphorylate PapA5 at Overlapping but Distinct Sites. Unexpectedly, PknB phosphorylation did not affect PapA5 activity *in vitro*. Although phosphorylated PapA5 was generated in a recombinant overexpression system, modification by PknB in this context appears to be specific, as phosphorylation was detected at only 3 of 28 Thr residues in PapA5, ~20 of which are at the protein surface. Interestingly, modified residues T196 and T198 are located in the middle of an unresolved region (aa 192–204) at the surface of PapA5 (Figure 5C). Along with T214, these residues encompass a region proximal to helix H and the entrance to the putative phthiocerol binding channel and may therefore modulate the interaction of PapA5 with other proteins (Figure 5C). The phosphorylation of T196 and T198 in particular supports this idea, as unstructured segments are common motifs in protein–protein interactions.[56] Enzymes that catalyze successive steps can form multiprotein complexes to promote efficient turnover and access to substrates, and interactions have been reported between the DIM transporter MmpL7 and PpsE, between PpsE and the PDIM-associated thioesterase TesA, and between the acyl carrier domain of mycocerosic acid synthase (Mas-ACP) and PapA5.[57−59] Residues implicated in the interaction with Mas-ACP (R234 and R312) are located on a facet orthogonal to T186, T198, and T214 (Figure 5B,C), suggesting that post-translational modification is unlikely to affect Mas binding.[59] Rather, phosphorylation of these residues may modulate PapA5 interactions with the negatively charged plasma membrane[1,60] or with other phthiocerol biosynthetic enzymes, particularly the terminal phthiocerol enzyme PpsE, with consequences for DIM levels in the cell. Interestingly, coexpression with PknE resulted in insoluble PapA5, perhaps due to the disruption of a hydrogen bond by phosphorylation at T144. While PknB and PknE modifications overlap at T196, T198, and T214, PknE phosphorylation may affect PapA5 stability by modifying T144 and thus regulate PapA5 in a manner distinct from PknB modification. These results, along with previous reports of MmpL7, Mas, and Pks1/15 phosphorylation, warrant further investigation into the potentially diverse roles of phosphorylation in modulating DIM biosynthesis.[30,32,33]

■ ASSOCIATED CONTENT

Supporting Information

The Supporting Information is available free of charge on the ACS Publications website at DOI: 10.1021/acs.biochem.5b00455.

Expression constructs and oligonucleotide primers used in this study (Table S1); PDD diester forms under aqueous conditions at high diol concentration (Figure S1); biphasic reaction conditions do not affect PapA5 activity with OCT (Figure S2); substrate-blocking mutations modulate PapA5 activity (Figure S3); circular dichroism of purified wild-type and mutant PapA5 (Figure S4) (PDF).

■ AUTHOR INFORMATION

Corresponding Author

*Tel: 631-632-1674; Fax: 631-632-1692; E-mail: jessica.seeliger@stonybrook.edu.

Funding

This work was supported by NIH CA58530 (W.T.M.), NIH GM102864 (P.J.T.), NSF CHE-1058439 (N.S.S.), and a Stony Wold–Herbert Foundation Grant-In-Aid (to J.C.S.). Protein mass spectrometric analysis was performed by the Proteomics Center at Stony Brook University and supported by NIH/NCRR 1 S10 RR023680-1. Lipidomics analyses were performed at the Environmental Molecular Sciences Laboratory, a national scientific user facility sponsored by the Department of Energy's Office of Biological and Environmental Research (OBER) and located at Pacific Northwest National Laboratory (PNNL). PNNL is a multiprogram national laboratory operated by Battelle for the Department of Energy (DOE) under Contract DE-AC05-76RLO 1830. Lipidomics analyses were enabled by capabilities developed by the PNNL Pan-omics Program under support from the DOE OBER Genome Sciences Program.

Notes

The authors declare no competing financial interest.

■ ACKNOWLEDGMENTS

We thank Mary Lou Previti for assistance with cloning and Bela Ruzsicska and the Stony Brook University Institute for Chemical Biology and Drug Discovery for assistance with mass spectrometry. We also gratefully acknowledge Christina Baer, Lauren Spagnuolo, and members of the Seeliger lab for helpful discussions.

■ ABBREVIATIONS

DHB, 2,5-dihydroxybenzoic acid; DIM, dimycocerosate; FASII, fatty acid synthase II; Mtb, *Mycobacterium tuberculosis*; OCT, 1-octanol; PCoA, palmitoyl-coenzyme A; PDD, (5*R*,7*R*)-pentadecane-5,7-diol; PDIM, phthiocerol dimycocerosate; PGL, phenolic glycolipid; PKS, polyketide synthase; RHD, 3*R*,5*R*-heptanediol; SHD, 3*S*,5*S*-heptanediol; TB, tuberculosis; TCEP, tris(2-carboxyethyl)phosphine; TLC, thin-layer chromatography; UDD, (5*R*,7*R*)-undecane-5,7-diol

■ REFERENCES

(1) Crellin, P. K., Luo, C.-Y., and Morita, Y. S. (2013) Metabolism of Plasma Membrane Lipids in Mycobacteria and Corynebacteria, in *Lipid Metabolism* (Baez, R. V., Ed.) pp 119–148, InTech, Rijeka, Croatia.

(2) Weidenmaier, C., and Peschel, A. (2008) Teichoic acids and related cell-wall glycopolymers in Gram-positive physiology and host interactions. *Nat. Rev. Microbiol. 6*, 276–287.

(3) Silhavy, T. J., Kahne, D., and Walker, S. (2010) The Bacterial Cell Envelope. *Cold Spring Harbor Perspect. Biol. 2*, a000414.

(4) Brennan, P. J., and Nikaido, H. (1995) The envelope of mycobacteria. *Annu. Rev. Biochem. 64*, 29–63.

(5) Daffe, M., and Laneelle, M. A. (1988) Distribution of phthiocerol diester, phenolic mycosides and related compounds in mycobacteria. *Microbiology 134*, 2049–2055.

(6) Goren, M. B., Brokl, O., and Schaefer, W. B. (1974) Lipids of putative relevance to virulence in Mycobacterium tuberculosis:

DOI: 10.1021/acs.biochem.5b00455
Biochemistry 2015, 54, 5457–5468

phthiocerol dimycocerosate and the attenuation indicator lipid. *Infect. Immun. 9*, 150−158.
(7) Cox, J. S., Chen, B., McNeil, M., and Jacobs, W. R., Jr. (1999) Complex lipid determines tissue-specific replication of Mycobacterium tuberculosis in mice. *Nature 402*, 79−83.
(8) Camacho, L. R., Ensergueix, D., Perez, E., Gicquel, B., and Guilhot, C. (1999) Identification of a virulence gene cluster of Mycobacterium tuberculosis by signature-tagged transposon mutagenesis. *Mol. Microbiol. 34*, 257−267.
(9) Yu, J., Tran, V., Li, M., Huang, X., Niu, C., Wang, D., Zhu, J., Wang, J., Gao, Q., and Liu, J. (2012) Both phthiocerol dimycocerosates and phenolic glycolipids are required for virulence of Mycobacterium marinum. *Infect. Immun. 80*, 1381−1389.
(10) Rousseau, C., Winter, N., Pivert, E., Bordat, Y., Neyrolles, O., Avé, P., Huerre, M., Gicquel, B., and Jackson, M. (2004) Production of phthiocerol dimycocerosates protects Mycobacterium tuberculosis from the cidal activity of reactive nitrogen intermediates produced by macrophages and modulates the early immune response to infection. *Cell. Microbiol. 6*, 277−287.
(11) Murry, J. P., Pandey, A. K., Sassetti, C. M., and Rubin, E. J. (2009) Phthiocerol Dimycocerosate Transport Is Required for Resisting Interferon-γ−Independent Immunity. *J. Infect. Dis. 200*, 774−782.
(12) Kirksey, M. A., Tischler, A. D., Siméone, R., Hisert, K. B., Uplekar, S., Guilhot, C., and McKinney, J. D. (2011) Spontaneous Phthiocerol Dimycocerosate-Deficient Variants of Mycobacterium tuberculosis Are Susceptible to Gamma Interferon-Mediated Immunity. *Infect. Immun. 79*, 2829−2838.
(13) Cambier, C. J., Takaki, K. K., Larson, R. P., Hernandez, R. E., Tobin, D. M., Urdahl, K. B., Cosma, C. L., and Ramakrishnan, L. (2014) Mycobacteria manipulate macrophage recruitment through coordinated use of membrane lipids. *Nature 505*, 218−222.
(14) Quadri, L. E. (2014) Biosynthesis of mycobacterial lipids by polyketide synthases and beyond. *Crit. Rev. Biochem. Mol. Biol. 49*, 179−211.
(15) Vergnolle, O., Chavadi, S. S., Edupuganti, U. R., Mohandas, P., Chan, C., Zeng, J., Kopylov, M., Angelo, N. G., Warren, J. D., Soll, C. E., and Quadri, L. E. (2015) Biosynthesis of mycobacterial cell-envelope-associated phenolic glycolipids in Mycobacterium marinum. *J. Bacteriol. 197*, 1040−1050.
(16) Chavadi, S. S., Onwueme, K. C., Edupuganti, U. R., Jerome, J., Chatterjee, D., Soll, C. E., and Quadri, L. E. N. (2012) The mycobacterial acyltransferase PapA5 is required for biosynthesis of cell wall-associated phenolic glycolipids. *Microbiology 158*, 1379−1387.
(17) Onwueme, K. C., Ferreras, J. A., Buglino, J., Lima, C. D., and Quadri, L. E. N. (2004) Mycobacterial polyketide-associated proteins are acyltransferases: Proof of principle with Mycobacterium tuberculosis PapA5. *Proc. Natl. Acad. Sci. U. S. A. 101*, 4608−4613.
(18) Buglino, J., Onwueme, K. C., Ferreras, J. A., Quadri, L. E. N., and Lima, C. D. (2004) Crystal Structure of PapA5, a Phthiocerol Dimycocerosyl Transferase from Mycobacterium tuberculosis. *J. Biol. Chem. 279*, 30634−30642.
(19) Camacho, L. R., Constant, P., Raynaud, C., Laneelle, M. A., Triccas, J. A., Gicquel, B., Daffe, M., and Guilhot, C. (2001) Analysis of the phthiocerol dimycocerosate locus of Mycobacterium tuberculosis. Evidence that this lipid is involved in the cell wall permeability barrier. *J. Biol. Chem. 276*, 19845−19854.
(20) Sulzenbacher, G., Canaan, S., Bordat, Y., Neyrolles, O., Stadthagen, G., Roig-Zamboni, V., Rauzier, J., Maurin, D., Laval, F., Daffé, M., Cambillau, C., Gicquel, B., Bourne, Y., and Jackson, M. (2006) LppX is a lipoprotein required for the translocation of phthiocerol dimycocerosates to the surface of *Mycobacterium tuberculosis*. *EMBO J. 25*, 1436−1444.
(21) Kumar, P., Schelle, M. W., Jain, M., Lin, F. L., Petzold, C. J., Leavell, M. D., Leary, J. A., Cox, J. S., and Bertozzi, C. R. (2007) PapA1 and PapA2 are acyltransferases essential for the biosynthesis of *Mycobacterium tuberculosis* virulence factor Sulfolipid-1. *Proc. Natl. Acad. Sci. U. S. A. 104*, 11221−11226.
(22) Bhatt, K., Gurcha, S. S., Bhatt, A., Besra, G. S., and Jacobs, W. R. (2007) Two polyketide-synthase-associated acyltransferases are required for sulfolipid biosynthesis in Mycobacterium tuberculosis. *Microbiology 153*, 513−520.
(23) Hatzios, S. K., Schelle, M. W., Holsclaw, C. M., Behrens, C. R., Botyanszki, Z., Lin, F. L., Carlson, B. L., Kumar, P., Leary, J. A., and Bertozzi, C. R. (2009) PapA3 is an acyltransferase required for Polyacyltrehalose biosynthesis in Mycobacterium tuberculosis. *J. Biol. Chem. 284*, 12745−12751.
(24) Jain, M., Petzold, C. J., Schelle, M. W., Leavell, M. D., Mougous, J. D., Bertozzi, C. R., Leary, J. A., and Cox, J. S. (2007) Lipidomics reveals control of Mycobacterium tuberculosis virulence lipids via metabolic coupling. *Proc. Natl. Acad. Sci. U. S. A. 104*, 5133−5138.
(25) Yang, X., Nesbitt, N. M., Dubnau, E., Smith, I., and Sampson, N. S. (2009) Cholesterol Metabolism Increases the Metabolic Pool of Propionate in Mycobacterium tuberculosis. *Biochemistry 48*, 3819−3821.
(26) Singh, A., Crossman, D. K., Mai, D., Guidry, L., Voskuil, M. I., Renfrow, M. B., and Steyn, A. J. C. (2009) *Mycobacterium tuberculosis* WhiB3Maintains Redox Homeostasis by Regulating Virulence Lipid Anabolism to Modulate Macrophage Response. *PLoS Pathog. 5*, e1000545.
(27) Shi, L., Sohaskey, C. D., Kana, B. D., Dawes, S., North, R. J., Mizrahi, V., and Gennaro, M. L. (2005) Changes in energy metabolism of Mycobacterium tuberculosis in mouse lung and under in vitro conditions affecting aerobic respiration. *Proc. Natl. Acad. Sci. U. S. A. 102*, 15629−15634.
(28) Rohde, K. H., Veiga, D. F., Caldwell, S., Balazsi, G., and Russell, D. G. (2012) Linking the transcriptional profiles and the physiological states of Mycobacterium tuberculosis during an extended intracellular infection. *PLoS Pathog. 8*, e1002769.
(29) Gomez-Velasco, A., Bach, H., Rana, A. K., Cox, L. R., Bhatt, A., Besra, G. S., and Av-Gay, Y. (2013) Disruption of the serine/threonine protein kinase H affects phthiocerol dimycocerosates synthesis in Mycobacterium tuberculosis. *Microbiology 159*, 726−736.
(30) Perez, J., Garcia, R., Bach, H., de Waard, J. H., Jacobs, W. R., Jr., Av-Gay, Y., Bubis, J., and Takiff, H. E. (2006) Mycobacterium tuberculosis transporter MmpL7 is a potential substrate for kinase PknD. *Biochem. Biophys. Res. Commun. 348*, 6−12.
(31) Gupta, M., Sajid, A., Arora, G., Tandon, V., and Singh, Y. (2009) Forkhead-associated domain-containing protein Rv0019c and polyketide-associated protein PapA5, from substrates of serine/threonine protein kinase PknB to interacting proteins of Mycobacterium tuberculosis. *J. Biol. Chem. 284*, 34723−34734.
(32) Prisic, S., Dankwa, S., Schwartz, D., Chou, M. F., Locasale, J. W., Kang, C. M., Bemis, G., Church, G. M., Steen, H., and Husson, R. N. (2010) Extensive phosphorylation with overlapping specificity by Mycobacterium tuberculosis serine/threonine protein kinases. *Proc. Natl. Acad. Sci. U. S. A. 107*, 7521−7526.
(33) Fortuin, S., Tomazella, G. G., Nagaraj, N., Sampson, S. L., Gey van Pittius, N. C., Soares, N. C., Wiker, H. G., de Souza, G. A., and Warren, R. M. (2015) Phosphoproteomics analysis of a clinical Mycobacterium tuberculosis Beijing isolate: expanding the mycobacterial phosphoproteome catalog. *Front. Microbiol. 6*, 6.
(34) Molle, V., Gulten, G., Vilcheze, C., Veyron-Churlet, R., Zanella-Cleon, I., Sacchettini, J. C., Jacobs, W. R., Jr., and Kremer, L. (2010) Phosphorylation of InhA inhibits mycolic acid biosynthesis and growth of Mycobacterium tuberculosis. *Mol. Microbiol. 78*, 1591−1605.
(35) Corrales, R. M., Molle, V., Leiba, J., Mourey, L., de Chastellier, C., and Kremer, L. (2012) Phosphorylation of mycobacterial PcaA inhibits mycolic acid cyclopropanation: consequences for intracellular survival and for phagosome maturation block. *J. Biol. Chem. 287*, 26187−26199.
(36) Vilcheze, C., Molle, V., Carrere-Kremer, S., Leiba, J., Mourey, L., Shenai, S., Baronian, G., Tufariello, J., Hartman, T., Veyron-Churlet, R., Trivelli, X., Tiwari, S., Weinrick, B., Alland, D., Guerardel, Y., Jacobs, W. R., Jr., and Kremer, L. (2014) Phosphorylation of KasB Regulates Virulence and Acid-Fastness in Mycobacterium tuberculosis. *PLoS Pathog. 10*, e1004115.

DOI: 10.1021/acs.biochem.5b00455
Biochemistry 2015, 54, 5457−5468

(37) Huang, G. F., and Hollingsworth, R. I. (1998) An efficient synthesis of (R)-3-hydroxytetradecanoic acid. *Tetrahedron: Asymmetry 9*, 4113−4115.
(38) Larcheveque, M., and Henrot, S. (1990) Enantiomerically Pure Beta,Gamma-Epoxyesters from Beta-Hydroxylactones - Synthesis of Beta-Hydroxyesters and (−)-GABOB. *Tetrahedron 46*, 4277−4282.
(39) Roche, C., Labeeuw, O., Haddad, M., Ayad, T., Genet, J. P., Ratovelomanana-Vidal, V., and Phansavath, P. (2009) Synthesis of anti-1,3-Diols through RuCl3/PPh3-Mediated Hydrogenation of beta-Hydroxy Ketones: An Alternative to Organoboron Reagents. *Eur. J. Org. Chem. 2009*, 3977−3986.
(40) Zorb, A., and Bruckner, R. (2010) Conversion of Conjugated Enones into Enantiomerically Pure beta-Hydroxy Ketones or 1,3-Diols - Samarium(II) Bromide Reductions of Protected alpha,beta-Dihydroxy Ketones. *Eur. J. Org. Chem. 2010*, 4785−4801.
(41) Evans, D. A., and Chapman, K. T. (1986) The Directed Reduction of Beta-Hydroxy Ketones Employing Me4NHB(OAc)3. *Tetrahedron Lett. 27*, 5939−5942.
(42) Casas-Arce, E., ter Horst, B., Feringa, B., and Minnaard, A. (2008) Asymmetric Total Synthesis of PDIM A: A Virulence Factor of Mycobacterium tuberculosis. *Chem. - Eur. J. 14*, 4157−4159.
(43) ter Horst, B., Feringa, B. L., and Minnaard, A. J. (2007) Catalytic Asymmetric Synthesis of Phthioceranic Acid, a Heptamethyl-Branched Acid from Mycobacterium tuberculosis. *Org. Lett. 9*, 3013−3015.
(44) Su, C. Y., London, E., and Sampson, N. S. (2013) Mapping peptide thiol accessibility in membranes using a quaternary ammonium isotope-coded mass tag (ICMT). *Bioconjugate Chem. 24*, 1235−1247.
(45) Gao, X., Zhang, Q., Meng, D., Isaac, G., Zhao, R., Fillmore, T., Chu, R., Zhou, J., Tang, K., Hu, Z., Moore, R., Smith, R., Katze, M., and Metz, T. (2012) A reversed-phase capillary ultra-performance liquid chromatography−mass spectrometry (UPLC-MS) method for comprehensive top-down/bottom-up lipid profiling. *Anal. Bioanal. Chem. 402*, 2923−2933.
(46) Baer, C. E., Iavarone, A. T., Alber, T., and Sassetti, C. M. (2014) Biochemical and spatial coincidence in the provisional Ser/Thr protein kinase interaction network of Mycobacterium tuberculosis. *J. Biol. Chem. 289*, 20422−20433.
(47) Evans, D. A., Chapman, K. T., and Carreira, E. M. (1988) Directed Reduction of Beta-Hydroxy Ketones Employing Tetramethylammonium Triacetoxyborohydride. *J. Am. Chem. Soc. 110*, 3560−3578.
(48) Grundner, C., Gay, L. M., and Alber, T. (2005) Mycobacterium tuberculosis serine/threonine kinases PknB, PknD, PknE, and PknF phosphorylate multiple FHA domains. *Protein Sci. 14*, 1918−1921.
(49) Sharma, K., Chandra, H., Gupta, P. K., Pathak, M., Narayan, A., Meena, L. S., D'Souza, R. C., Chopra, P., Ramachandran, S., and Singh, Y. (2004) PknH, a transmembrane Hank's type serine/threonine kinase from Mycobacterium tuberculosis is differentially expressed under stress conditions. *FEMS Microbiol. Lett. 233*, 107−113.
(50) Hsiao, Y. S., Jogl, G., and Tong, L. (2004) Structural and biochemical studies of the substrate selectivity of carnitine acetyltransferase. *J. Biol. Chem. 279*, 31584−31589.
(51) Mattevi, A. (2006) A monotopic membrane protein goes solo. *Structure 14*, 628−629.
(52) Rufer, A. C., Lomize, A., Benz, J., Chomienne, O., Thoma, R., and Hennig, M. (2007) Carnitine palmitoyltransferase 2: analysis of membrane association and complex structure with a substrate analog. *FEBS Lett. 581*, 3247−3252.
(53) Perspicace, S., Rufer, A. C., Thoma, R., Mueller, F., Hennig, M., Ceccarelli, S., Schulz-Gasch, T., and Seelig, J. (2013) Isothermal titration calorimetry with micelles: Thermodynamics of inhibitor binding to carnitine palmitoyltransferase 2 membrane protein. *FEBS Open Bio 3*, 204−211.
(54) Carel, C., Nukdee, K., Cantaloube, S., Bonne, M., Diagne, C. T., Laval, F., Daffe, M., and Zerbib, D. (2014) Mycobacterium tuberculosis proteins involved in mycolic acid synthesis and transport localize dynamically to the old growing pole and septum. *PLoS One 9*, e97148.
(55) Meniche, X., Otten, R., Siegrist, M. S., Baer, C. E., Murphy, K. C., Bertozzi, C. R., and Sassetti, C. M. (2014) Subpolar addition of new cell wall is directed by DivIVA in mycobacteria. *Proc. Natl. Acad. Sci. U. S. A. 111*, E3243−3251.
(56) Neduva, V., and Russell, R. B. (2005) Linear motifs: evolutionary interaction switches. *FEBS Lett. 579*, 3342−3345.
(57) Jain, M., and Cox, J. S. (2005) Interaction between polyketide synthase and transporter suggests coupled synthesis and export of virulence lipid in M. tuberculosis. *PLoS Pathog. 1*, e2.
(58) Rao, A., and Ranganathan, A. (2004) Interaction studies on proteins encoded by the phthiocerol dimycocerosate locus of Mycobacterium tuberculosis. *Mol. Genet. Genomics 272*, 571−579.
(59) Trivedi, O. A., Arora, P., Vats, A., Ansari, M. Z., Tickoo, R., Sridharan, V., Mohanty, D., and Gokhale, R. S. (2005) Dissecting the Mechanism and Assembly of a Complex Virulence Mycobacterial Lipid. *Mol. Cell 17*, 631−643.
(60) Thelen, M., Rosen, A., Nairn, A. C., and Aderem, A. (1991) Regulation by phosphorylation of reversible association of a myristoylated protein kinase C substrate with the plasma membrane. *Nature 351*, 320−322.

DOI: 10.1021/acs.biochem.5b00455
Biochemistry 2015, 54, 5457−5468